PERGAMON

Carbon 39 (2001) 523–534

CARBON

Effects of pore structure and temperature on VOC adsorption on activated carbon

Yu-Chun Chiang[a,*], Pen-Chi Chiang[b], Chin-Pao Huang[c]

[a]*Department of Mechanical Engineering, Yuan Ze University, 135 Yuan-Tung Rd., Chung-Li, Taoyuan, Taiwan*
[b]*Graduate Institute of Environmental Engineering, National Taiwan University, 71 Chou-Shan Rd., Taipei, Taiwan*
[c]*Department of Civil and Environmental Engineering, University of Delaware, Newark, DE 19716, USA*

Received 19 February 2000; accepted 9 June 2000

Abstract

This research was undertaken to investigate the pore structure of three activated carbons and determine the temperature dependence of the adsorption of VOCs onto activated carbon. Three kinds of activated carbon made of different raw materials and four VOC species were chosen. The microporosity of activated carbon was assessed by the pore size distribution. The adsorption of VOCs showed that only C_6H_6 exhibited the activated entry effect. The VOC adsorption capacity of peat-derived carbon was less dependent on temperature. A characteristic curve was observed for the peat-derived carbon. Benzene adsorption was the most preferable compared to other three VOCs because of higher heats of adsorption and lower entropy change. Results indicate physical adsorption played a critical role during adsorption processes in this study system.

Keywords: A. Activated carbon; C. Adsorption, BET surface area; D. Porosity, Thermodynamic properties

1. Introduction

Due to ubiquity in the environment and risk to human health, volatile organic compounds (VOCs) have received great attention in the field of environmental control. The adsorption of VOCs onto porous adsorbents, such as activated carbons, has been suggested as an innovative treatment technology. Activated carbon adsorption has been considered to be one of the promising methods for controlling VOCs of low concentrations with potential to recover valuable vapors. Activated carbon characterized with heterogeneously porous structures, generally, can be made from a variety of raw materials such as peat, coal, nut shell, lignite, saw dust, and synthetic polymers.

The adsorption capacity of activated carbon depends strongly on its surface microstructure. Consequently, information on the surface characteristics of activated carbon is important to adsorption process design. To date, adsorption isotherms of inert gases, such as nitrogen and argon, are the most widely used to determine the physical structure of porous activated carbons. According to the BET classification of isotherm, in general, adsorption on porous solids would belong to the Type IV isotherm [1], which is characterized by a hysteresis loop. de Boer [2] first proposed five major distinct hysteresis loops. The IUPAC (International Union of Pure & Applied Chemistry) later recommended a different classification system and categorized hysteresis loops into four groups, Type H1, H2, H3 and H4 [3]. The lower closure point of the hysteresis loop occurs at a relative pressure which is almost independent of the nature of adsorbent but mainly relies on the properties of the adsorbate. For example, it occurs at $P/P_o \fallingdotseq 0.42$ for nitrogen at 77 K and at $P/P_o \fallingdotseq 0.28$ for benzene at 298 K [4].

The profile of hysteresis loop is closely related to both the shapes of pores and the pore size distribution. Kelvin was the first to calculate the pore size using a cylindrical model [1]. However, the Kelvin equation is only applicable in the range of $P/P_o > 0.42$. In order to predict the pore size distribution under low pressure conditions, Lippens and de Boer [5] developed the t-method which was later modified by Mikhail et al. [6] proposing the micropore method, MP-method. Horvath and Kawazoe [7] based on the concept of average potential function, developed a slit

*Corresponding author. Tel.: +886-3-463-8800 ext. 476; fax: +886-3-455-8013.

E-mail address: ycchiang@saturn.yzu.edu.tw (Y.-C. Chiang).

0008-6223/01/$ – see front matter
PII: S0008-6223(00)00161-5

model for predicting the pore size distribution in micropore carbons; however, the model failed to predict the pore size distribution of larger pores.

Gas adsorption at the solid surface is a spontaneous process when the change in free energy, ΔG, of the system decreases. Since the adsorbed gas is less mobile than its gaseous state, the entropy change, ΔS, is negative [8]. At a given relative pressure and under most circumstances, the amount of gas adsorbed decreases with increasing temperature. However, some researchers have observed that the adsorbed amount at a given temperature is larger than that measured at a lower temperature in the same gas/solid system. This behavior, defined as the activated entry effect, is responsible for the temperature-dependent nature of equilibrium adsorption [9]. This abnormal phenomenon is speculated as caused by the diffusion of gas molecules through narrow constrictions into micropores, where the rate of entry into the pores will have a positive temperature coefficient. At a sufficiently high temperature, the approach to equilibrium will be fast enough so that the gas uptake will decrease as the temperature increases.

At constant pressure the heat evolved is usually considered the heat of adsorption, ΔH, which is also a measurement of the interactions between adsorbate molecules and adsorbent lattice atoms. The heat of adsorption is associated with the adsorption equilibrium constant, K, by the van't Hoff equation:

$$K = K_0 \exp\left(-\frac{\Delta H}{RT}\right) \quad (1)$$

Note that Eq. (1) is applicable to ideal gas only. Consequently, by plotting K against $1/T$, ΔH can be determined. Chihara et al. [10] found that there was a linear relationship between the heats of adsorption and the carbon numbers in the hydrocarbon-activated carbon adsorption system. In addition, it was reported that the heat of adsorption in molecular sieve carbon (MSC) was 2.6 times to the heats of vaporization of the corresponding adsorbate [10]. This value was twice as large as that of graphitized thermal carbon black. The result can be attributed to the enhanced interactions between the adsorbates and the carbon layers in MSC.

Findenegg and Liphard [11] studied the adsorption of higher n-alkanes (C_{16}–C_{32}) from dilute solutions of nonpolar organic solvents onto graphitized carbon. They found that the enthalpy of adsorption was a function of the fraction of surface covered. Meanwhile, the enthalpy of adsorption increased at higher surface concentration due to lateral interactions from close-packed adsorbates. Tsai [12] observed the temperature effect on the adsorption of chlorinated volatile organic compounds and suggested that when the temperature increased from 283 to 313 K and at an inflow concentration of 440 ppm, the uptake of methylene chloride on activated carbon BPL was reduced by 60%. Chiang [13] investigated the temperature dependence of benzene adsorption on coconut shell-derived carbon modified by ozonation. It was reported that when the temperature increased from 283 to 393 K and at an inflow concentration of 5000 ppm, the uptake of benzene on non-modified carbon was reduced by 28% only, while that on the modified carbon was decreased by 40%. Apparently, the modified activated carbon has larger micropore volume; therefore, it is temperature-dependent.

Temperature plays an important role on the design of adsorption system. This research was initiated to study the temperature dependence of the adsorption of volatile organic compounds (VOCs) by various activated carbon adsorbents. It was also to determine the thermodynamic parameters, such as heat of adsorption and entropy change, for different gas/solid systems, as a means to shed light on the mechanisms of the adsorption process.

2. Experimental methods

2.1. Materials

Three different types of activated carbon made of different raw materials were used in this study. Sorbonorit 3 (designated as carbon A), a peat-derived carbon from Norit (Netherlands), is pelletized and has a diameter of 3 mm. Filtrasorb 400 (designated as carbon B), supplied by Calgon (Pittsburgh, USA) and made of bituminous coal, is granular with a size of 12/40 mesh (0.915 mm). Unicarb (designated as carbon C), a coconut shell-derived carbon of granular form with a size of 4/8 mesh (3.57 mm), is provided by Liangchien (Taiwan). All activated carbon samples were pretreated at 250°C in an oven purged with pure nitrogen gas in vacuo overnight for removing the moisture and other contaminants prior to experiments. A total of four volatile organic compounds including carbon tetrachloride (CCl_4), chloroform ($CHCl_3$), benzene (C_6H_6), and methylene chloride (CH_2Cl_2) were studied. Carbon tetrachloride and benzene are typically non-polar and inert compounds, and have been extensively studied. Both chloroform and methylene chloride are common polar volatile chemical derivatives of carbon tetrachloride. Table 1 summarises some chemical properties of those adsorbates.

2.2. Methods

2.2.1. Adsorption isotherms of inert gases

Adsorption isotherms of nitrogen and argon, as well as the amount of mercury intrusion were obtained as to analyze the surface structure characteristics of activated carbon. Adsorption isotherms of nitrogen and argon gases were measured using the ASAP 2000 system (accelerated surface area and porosimetry system, V2.02, 1992). Before measurements, the activated carbon samples were degassed at 250°C. To determine the characteristics of macro- and

Table 1
Summary of the characteristics of adsorbates

Adsorbate	CAS No.	Molecular weight	Boiling point (K)	Dipole moment (Debyes)	Liquid density (g cm^{-3})	Cross sectional area (nm^2)
CCl_4	56-23-5	153.82	349.9	0	1.584 (298 K)	0.32
$CHCl_3$	67-66-3	119.38	334.3	1.1	1.489 (293 K)	0.28
C_6H_6	71-43-2	78.11	353.2	0	0.885 (289 K)	0.43
CH_2Cl_2	75-09-2	84.93	313.0	1.8	1.317 (298 K)	0.25

meso-pores (>2 nm), adsorption–desorption isotherm of the nitrogen gas at 77 K was recorded against different relative pressures, lasting about 12 h. A similar experimental approach was also employed for the analysis of micropores (<2 nm) except replacing the nitrogen gas with the argon gas. At relative pressures were below 0.001, the adsorption isotherm was obtained by an active mode using 3.00 cm^3 g^{-1} dose amount (ASAP 2000, V3.00, 1993). In addition, the amounts of mercury intrusion into pores were measured with a mercury porosimeter, Autopore II 9220 V1.05. The mercury has a contact angle of 130 degrees and the surface tension of 485 dyne cm^{-1}. The range of applied pressure was from 0 to 380 MPa [14].

2.2.2. Density analysis

The determinations of density followed the procedures of Smisek [15] and Jankowska [16]. The true density (ρ_{He}) of activated carbon was determined by gas pycnometer (Accupyc 1330, Micromeritics), using helium gas at a pressure of 20 psia. An activated carbon sample (10 cm^3) was weighted and pre-conditioned several times with helium gas before measurements. Then the mean value of 10 runs for each sample was calculated. The apparent density (ρ_{Hg}) of activated carbon was analyzed utilizing mercury intrusion technology, which was based on the assumption that mercury does not penetrate into the pores with a diameter less than 15,000 nm at 1 atm. The apparatus of this method was simple and easy to operate, but the result was slightly dependent on the shape of activated carbons. Once the true density and apparent density were determined, the total pore volume (V_{pore}) and porosity (ϵ) could be determined by the following equations:

$$V_{pore} = \frac{1}{\rho_{Hg}} - \frac{1}{\rho_{He}} \quad (2)$$

$$\epsilon = 1 - (\rho_{Hg}/\rho_{He}) \quad (3)$$

2.2.3. VOCs adsorption experiments

The VOC adsorption experiments followed the ASTM D3467-94 method for the determination of carbon tetrachloride activity [17]. A given amount of activated carbon (ca. 300 mg) was weighed and placed into a U-shaped glass tube. The adsorption temperature, ranging from 278 to 353 K, was controlled by a water bath. The pure liquid adsorbate, contained in a volumetric flask, was immersed in a separate water bath. Purging the nitrogen gas over the pure liquid adsorbate generated the VOC vapor continuously. The VOC concentration depended on the flow rate of the nitrogen gas and the temperature of the water bath. The VOC concentration was monitored by gas chromatography with a flame ionization detector (HP 5890 serious II with a VOCOL™ capillary column). In this study, the concentration of VOCs was controlled at about 400 ppmv. The nitrogen gas carried the VOC vapor into the U-shaped glass tube containing weighted activated carbon sample. The contact time of VOC vapor and activated carbon sample was 24 h [18]. The amount VOC adsorbed was determined by weighing the activated carbon sample before and after adsorption process. The relative standard deviation of this experimental procedure was about 5.4%.

3. Results and discussion

3.1. Adsorption isotherms of nitrogen

Fig. 1 shows the adsorption–desorption isotherms of nitrogen at 77 K on carbons A, B and C. All isotherms exhibit a Type IV profile according to the BET classification. Each isotherm shows a distinct hysteresis loop, which is characteristic of porous adsorbents. This phenomenon is associated with capillary condensation in mesopores [19]. The lower end of the hysteresis loop in each isotherm approximately occurs at a relative pressure of 0.4, in accordance with the findings reported in literature [4]. It also means that the capillary condensation might start from the pore size at about 3 nm. The hysteresis loop of carbon B is significantly indicative of Type H3 profile, which is associated with aggregates of plate-like particles or slit-shaped pores. The Type H4 loop occurs in the isotherms of Carbon A and Carbon C, which explicates the nature of their narrow slit-like pores. The isotherms reveal that multilayer adsorption in Carbon A is not so significant as in Carbon B. On the other hand, having a Langmuir-type isotherm, nitrogen adsorption on Carbon C is approximately monolayer. Accordingly, it is speculated that Carbon A provides an excellent adsorption capacity; Carbon B

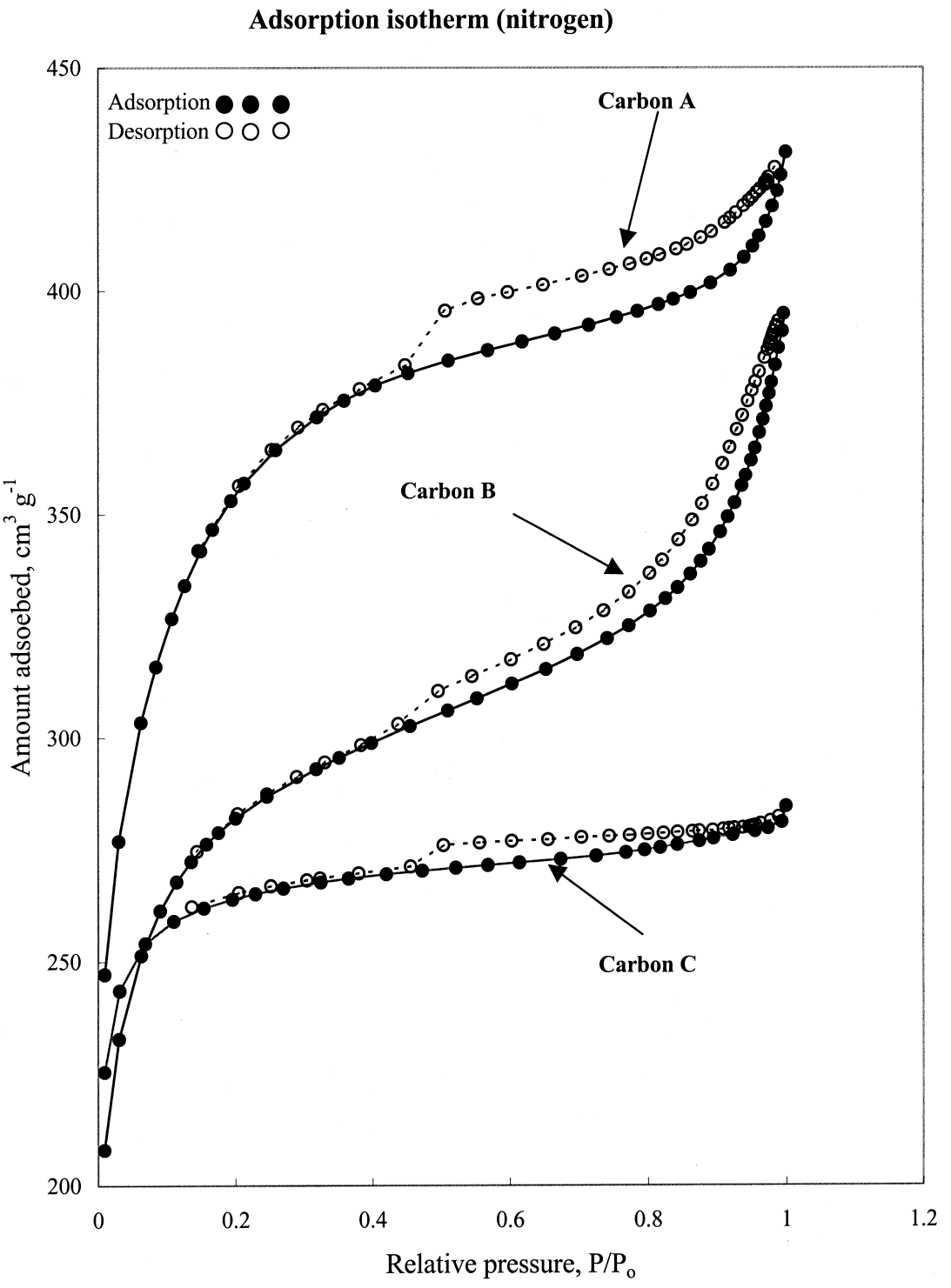

Fig. 1. Adsorption isotherms of nitrogen gas on activated carbons at 77 K.

should have a larger mean pore size; Carbon C has a narrow pore size distribution and a small mean pore size.

3.2. Surface area

Table 2 gives the specific surface areas of activated carbons calculated by various equations, e.g., BET and Langmuir. It was observed that the BET equation only applied in the range of relative pressure of $P/P_o < 0.14$. This finding implies that the pore size distribution might be skew toward to the smaller end. The C values of the BET equation for all carbons are greater than 100. Wherein the coconut shell-derived carbon (Carbon C), having a specific surface area of 975 $m^2\ g^{-1}$, has the highest C value of 761 over a range of relative pressures from 0.01 to 0.08. The C value is related to the enthalpy of adsorption in the first adsorbed layer. Although it does not give a quantitative measurement of the enthalpy of adsorption, it is an indication of the magnitudes of the adsorbent–adsorbate interaction energy [4]. Apparently, the interaction energy between the adsorbent and adsorbate for Carbon C is stronger than Carbon A. This observation could be interpreted by the microporosity of Carbon C which is made from coconut shell as indicated by the sharp knee in the isotherm. The Langmuir equation only describes mathematically Type I isotherms. Therefore, only for Carbon C can it make sense. Table 2 also shows the ratio of the monolayer adsorbed amount obtained from the BET equation to that obtained from the Langmuir equation for Carbon C. This ratio is close to unity, which indicates that micropores contribute the primary adsorption capacity of Carbon C with a narrow pore size distribution. This is consistent with the above-mentioned findings.

3.3. Characteristics of porosity

Since none of the current methods is capable of providing a measurement of the pore size distribution over the whole relative pressure range, an integrated approach consisting of the Horvath and Kawazoe (H–K) method, the Kelvin equation and the mercury porosimetry was used. Table 3 gives details of surface pore characteristics of activated carbons. It is seen that Carbon B has a broad pore volume distribution. However, the pore volumes of micropore and mesopore of Carbons A and C are much predominant than their macropore volumes. Specifically, the percentage of micropore volume of Carbon C was 84%. This is indicative of the microporosity. Due to high mesopore and macropore volumes, Carbon B possesses a large mean pore size. The mesopore volume appears to be associated with the size profile of the hysteresis loop, which suggests that the capillary condensation should be in mesopores. Generally, the sum of the percentages of micropore and mesopore volumes for all three carbons exceeds 95%, which should bring about Langmuir isotherm. Furthermore, the nature of porosity was determined by the measurements of true density and apparent density (Table 3). It is noted that the apparent density of Carbon B is high at 1.25 g cm^{-3} and its total pore volume is only 0.344 $cm^3\ g^{-1}$, which makes Carbon B different from the other two carbons. Because of smaller particle sizes, this might be attributed to the fact that the capillary condensation in the inter-particles gives extra capacities for mercury intrusion. Consequently, the bituminous coal-derived carbon has a broader pore size distribution, the coconut shell-derived carbon is obviously microporous, and the peat-derived carbon has a marked adsorption capacity due to its high pore volume.

3.4. Activated entry effect

Fig. 2 shows clearly that at a given VOC concentration, the VOC adsorbed amount decreases as the temperature increases. Fig. 2(a) illustrates the benzene adsorption on three activated carbons. It is noted that for all three activated carbons, there exists an adsorption hill at the temperature of about 313 K. However, in the case of CCl_4, $CHCl_3$ and CH_2Cl_2, as shown in Fig. 2(b), this adsorption hill was absent. Benzene is a disc-like molecule [20] with a cross-sectional area of 0.43 nm^2 which is apparently

Table 2
Summary of specific surface areas of three activated carbons and the related information calculated from BET and Langmuir equations[a]

Activated carbon	BET method				Langmuir method[b]		V_{mB}/V_{mL}
	P/P_o range	S_B[c] ($m^2\ g^{-1}$)	C	V_{mB}[d] ($cm^3\ g^{-1}$)	S_L[e] ($m^2\ g^{-1}$)	V_{mL}[f] ($cm^3\ g^{-1}$)	
Carbon A	0.05–0.14	1472	126	397	–	–	–
Carbon B	0.05–0.12	1027	361	277	–	–	–
Carbon C	0.01–0.08	975	761	263	1196	323	0.81

[a] The parameter estimations are determined by the adsorption isotherms of argon gas.
[b] Applied to Carbon C only.
[c] S_B: The specific surface area calculated from the BET equation.
[d] V_{mB}: Monolayer adsorption capacity calculated from the BET equation.
[e] S_L: The specific surface area calculated from the Langmuir equation.
[f] V_{mL}: Monolayer adsorption capacity calculated from the Langmuir equation.

Table 3
Summary of surface pore characteristics of activated carbons

Activated carbon	Pore volume ($cm^3\ g^{-1}$)				Mean pore size[e], ω (nm)	True density,	Apparent density,	V_{pore}[f] ($cm^3\ g^{-1}$)	Porosity[g] ϵ (%)
	V_{micro}[a]	V_{meso}[b]	V_{macro}[c]	V_{total}[d]		ρ_{He} (g cm^{-3})	ρ_{He} (g cm^{-3})		
Carbon A	0.515 (66%)	0.255 (32%)	0.015 (2%)	0.785	1.524	2.27	0.88	0.697	61
Carbon B	0.380 (57%)	0.258 (39%)	0.028 (4%)	0.665	1.794	2.19	1.25	0.344	43
Carbon C	0.353 (84%)	0.057 (14%)	0.007 (2%)	0.417	1.394	2.07	0.99	0.525	52

[a] Micropore volume estimated from Horvath and Kawazoe method.
[b] Mesopore volume estimated from Kelvin equation.
[c] Macropore volume estimated from mercury intrusion method.
[d] Total pore volume summed up by V_{micro}, V_{meso} and V_{macro}.
[e] Mean pore size calculated from the equation of $\omega = 4 \times (V_{total}/S_L)$.
[f] Pore volume calculated from the equation of $V_{pore} = 1/\rho_{Hg} - 1/\rho_{He}$.
[g] Porosity calculated from the equation of $\epsilon = 1 - \rho_{Hg}/\rho_{He}$.

different from the molecular structure of the other compounds [21]. As a result, this adsorption hill occurred on benzene adsorption could be attributed to the activated entry effect. Specifically, the rise in temperature facilitates the diffusion of benzene molecules, which helps to propel the benzene molecules through narrow constrictions in the micropore network. Subsequently, the adsorption capacity is enhanced.

3.5. Adsorption characteristic curve

Since liquid-like condensation plays a role in VOC adsorption on activated carbon, the boiling point of VOC would be an important factor. Fig. 3(a) gives a plot of $(W - W_b)/W_b$ versus $(T - T_b)/T_b$ for the adsorption of benzene onto three activated carbons. Results indicate that there is a distinct divergence in the lower temperature ranges for benzene adsorption. Since chemical adsorption could be negligible at low temperatures, the surface structural characteristics of activated carbon should be the major factor controlling the adsorption process. Fig. 3(b) shows the adsorption of four selected VOCs onto Carbon A using the plot of $(W - W_b)/W_b$ *v*ersus $(T - T_b)/T_b$, and the observations are induced to a characteristic curve. From this characteristic curve, it is possible to predict the adsorption density of VOC by a specific activated carbon at any temperature.

It is further noted that the dimensionless temperature with respect to boiling point is not readily available for multi-component systems due to lack of information on the lump of boiling points of VOCs. Consequently, the dimensionless temperature with respect to the room temperature (298 K) is intended. Fig. 4 gives plots of $(W - W_{298})/W_{298}$ *v*ersus $(T - T_{298})/T_{298}$. It is noted that in the low temperature range, benzene adsorption on activated carbons is independent of the type of activated carbon. For example, at 278 K the amounts of benzene adsorbed on activated carbons were almost twice as those at 298 K, regardless of the types of activated carbon. This can be attributed to physical adsorption being predominant in low temperature ranges. However, in high temperature ranges, chemical interactions between activated carbon and VOC take place. The adsorptive capacity of carbon A (the peat-derived carbon) was markedly superior to other carbons, e.g., carbon C (the coconut shell-derived carbon). As mentioned above, Carbon C has a micropore volume greater than that of carbon A. It was also found that the adsorbed amount of VOC on carbon A was inversely proportional to the dipole moment especially at high temperatures. Consequently, the more polar the adsorbate, the greater the adsorbed amount is affected by temperature.

3.6. Thermodynamic parameters

Fig. 5(a) presents the van't Hoff plots of benzene adsorption. Two distinct linear segments were identified in the low temperature range from 278 K to 303 K and the high temperature region from 318 K to 353 K. In the low temperature range, the heat of benzene adsorption on carbon B was the highest and almost twice as that of adsorption on carbon C. For carbons A and B, the heat of adsorption was nearly identical in the two temperature regions. But for activated carbon C, the heat of adsorption in the high temperature region was obviously greater than that in the low temperature. The result implies that the adsorption potential for the carbons with predominant micropores is greatly increased at high temperatures. However, the heats of adsorption for CCl_4, $CHCl_3$ and CH_2Cl_2 on Carbon A remain constant over the whole temperature range [Figs. 5(b)].

Table 4 lists the heats of adsorption and entropy changes for the adsorption processes of VOCs onto activated

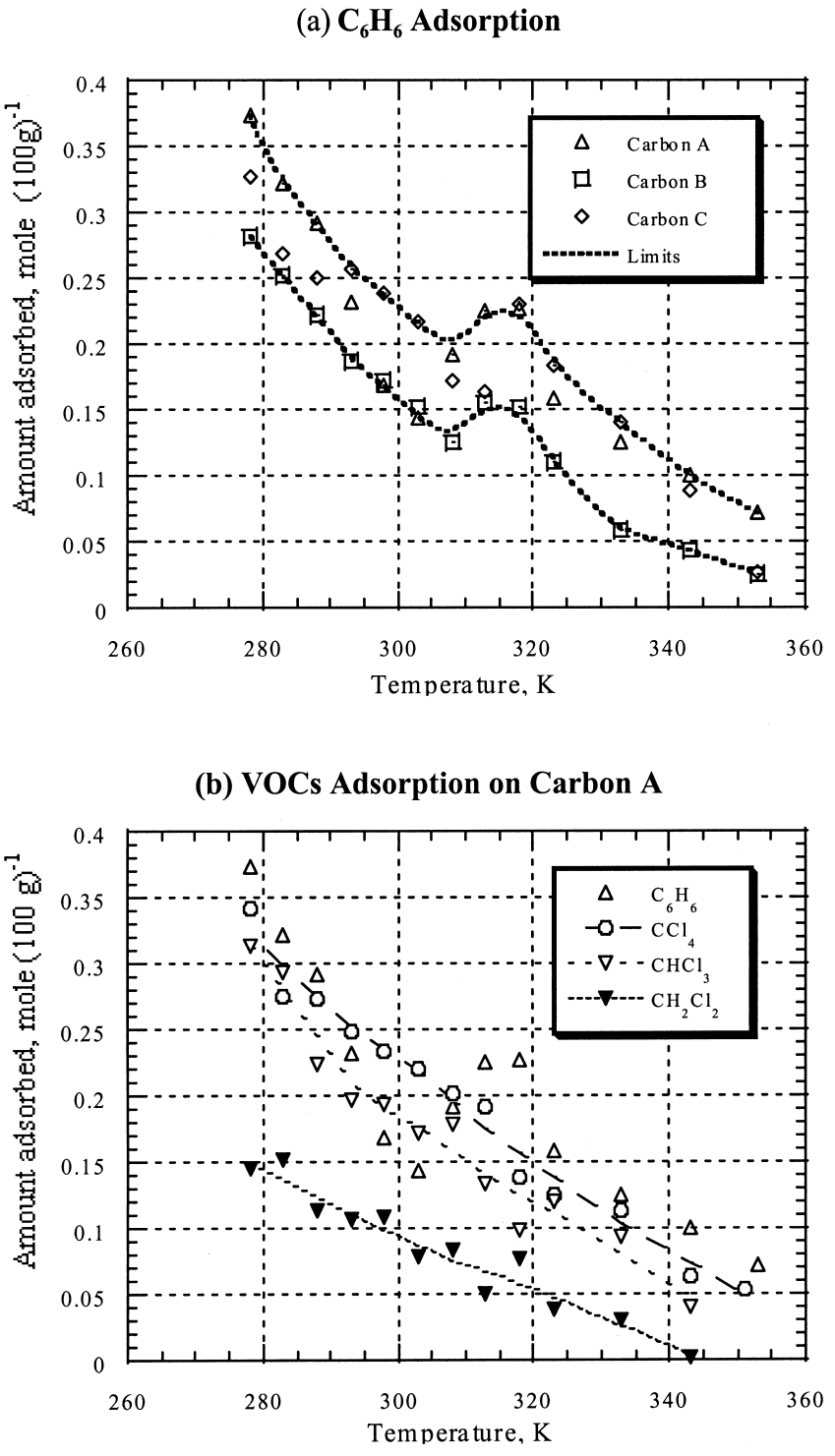

Fig. 2. VOCs adsorption on activated carbons as affected by temperature. Note: VOC concentration was about 1.7×10^{-5} mol l^{-1} at 298 K.

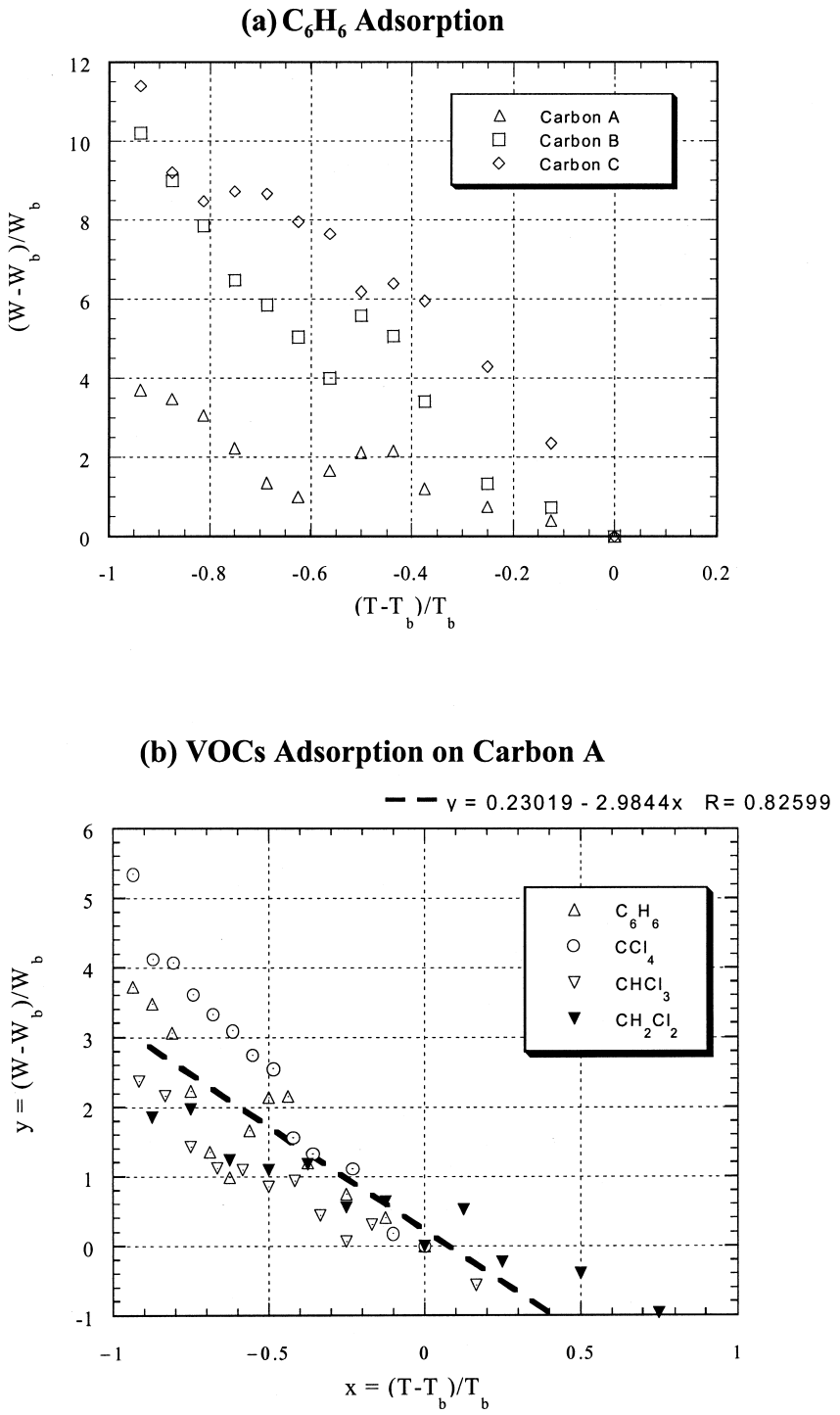

Fig. 3. Dimensionless plot of adsorption density (W) versus temperature (T) based on the boiling point of VOC (T_b). Note: W_b is the adsorption density at T_b. VOC concentration was about 1.7×10^{-5} mol l^{-1} at 298 K.

carbons. The difference in adsorption energy between benzene and other selected VOCs may be related to the non-equilibrium adsorption of benzene caused by activated entry effect. Generally, a high heat of adsorption means strong interactions between the adsorbent and adsorbate molecules. In the high temperature region, although ben-

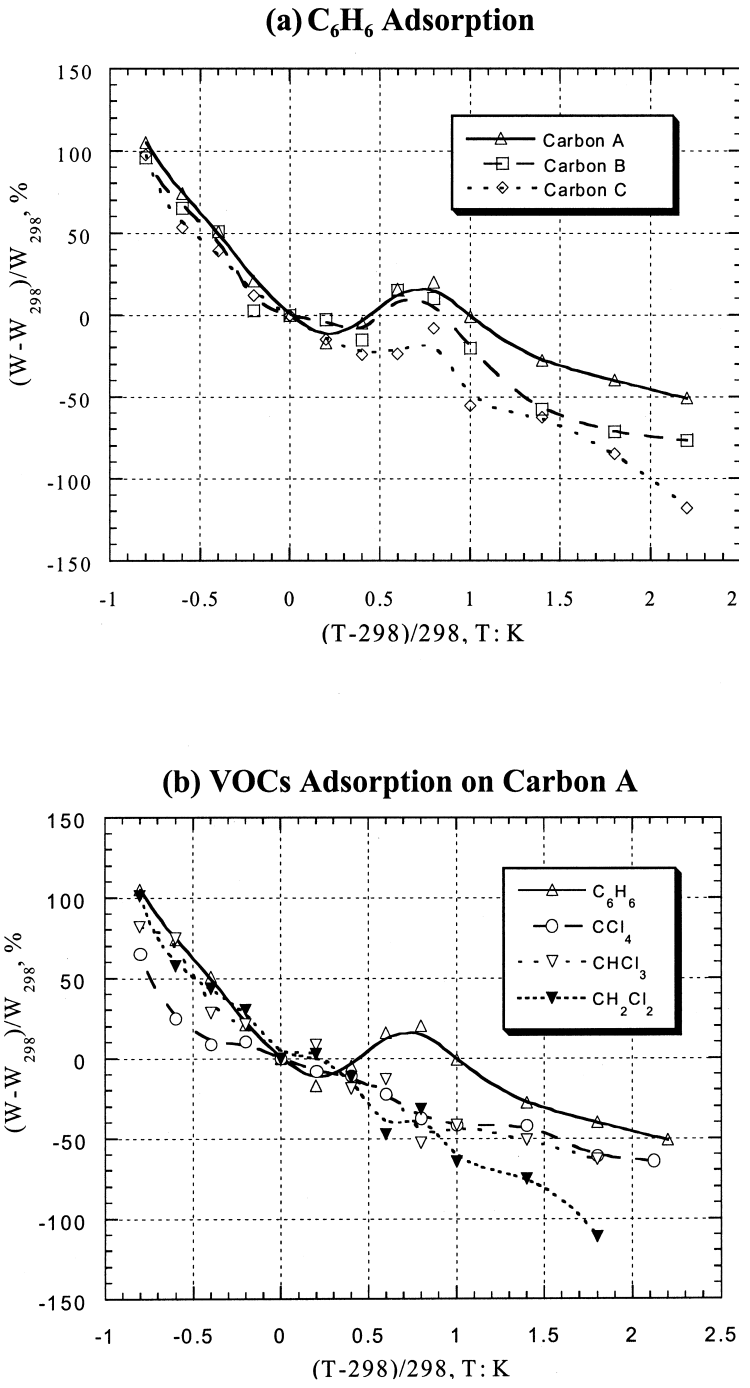

Fig. 4. Dimensionless plot of adsorption density (W) versus temperature (T) based on room temperature (298 K). Note: W_{298} is the adsorption density at 298 K. VOC concentration was about 1.7×10^{-5} mol l^{-1} at 298 K.

zene adsorption on carbons B and C yields high heat of adsorption, their adsorption capacities are less than that on carbon A. This clearly shows that physical adsorption plays an important role on benzene adsorption. In the adsorption of C_6H_6, CCl_4, $CHCl_3$ and CH_2Cl_2 on carbon A, the heats of adsorption are close to 40 kJ mol^{-1} which implies physical adsorption as the predominant mechanism for adsorption processes.

Table 4 also shows the change of entropy for each system. It was observed that the adsorbed amount was

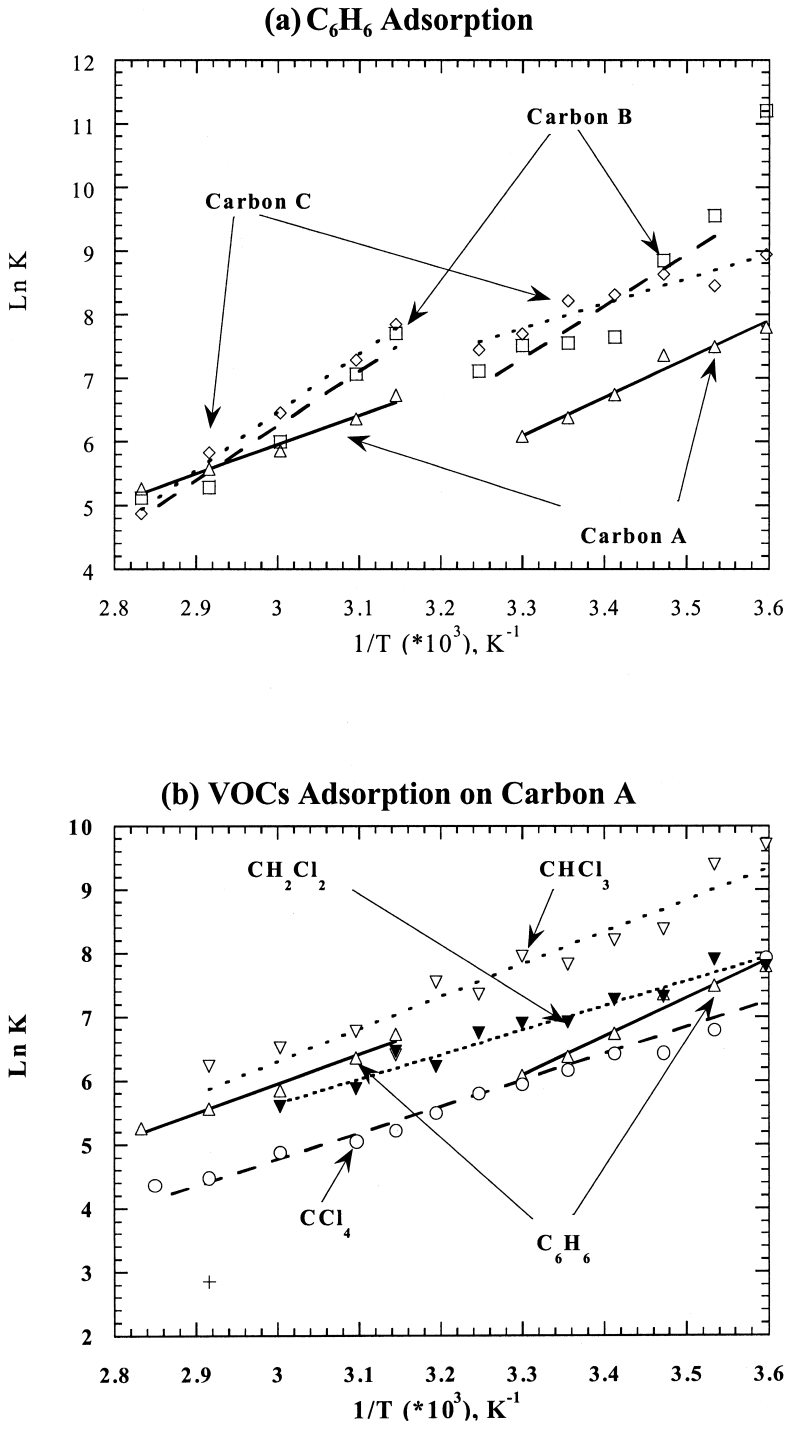

Fig. 5. Van't Hoff plots of VOC adsorption on activated carbons. (a) Benzene adsorption on three activated carbons. (b) Four VOC adsorption on carbon A.

related to the entropy change. For the adsorption of benzene on activated carbon A, the entropy change in the high temperature region was smaller than that in the low temperature region. This is consistent with the general premise that the system becomes more energetic when the temperature increases. In the case of benzene adsorption on

Table 4
Summary of thermodynamic parameters regarding the VOCs adsorption on activated carbons

Activated carbon	VOC	$-\Delta H_r$ (kJ mole^{-1})			$-\Delta S$ (kJ K^{-1} mole^{-1})		
		I (low T)	II (high T)	III (whole)	I (low T)	II (high T)	III (whole)
B	C_6H_6	68.41	71.13	–	0.163	0.163	–
C	C_6H_6	32.84	76.36	–	0.042	0.176	–
A	C_6H_6	50.12	38.03	–	0.113	0.063	–
A	CCl_4	–	–	34.43	–	–	0.063
A	$CHCl_3$	–	–	42.13	–	–	0.075
A	CH_2Cl_2	–	–	31.71	–	–	0.050

activated carbon B, the entropy change before and after adsorption processes was not sensitive to temperature. However, for the case of benzene adsorption on activated carbon C, the heat of adsorption increased twice and the entropy change also increased when the temperature increased. This was indicative of increasing the degree of interactions between benzene and carbon C as temperature increased. At the meantime, the system gradually approached to steady state. Nevertheless, the benzene adsorption decreased significantly which implied that physical adsorption was predominant mechanism. For CCl_4, $CHCl_3$ and CH_2Cl_2, the higher the degree of chlorine substitution, the less the dipole moment. The heat of adsorption or entropy change for these VOCs on Carbon A did not change in order of their properties, however.

Benzene adsorption was more preferable than other VOC species as indicated by its large heat of adsorption and entropy change. The vibrations of heat of adsorption and entropy change caused by temperature change suggest that physical adsorption is the predominant VOC adsorption mechanism. However, results also reveal an enhancement of interactions between VOC species and activated carbons in the high temperature range.

4. Conclusions

The adsorption–desorption isotherms of nitrogen gas implies that the nature of the pores on bituminous coal-derived carbon was slit-shaped capillaries or resulted from aggregates of the plate-like particles; however, the peat-derived carbon and the coconut shell-derived carbon possessed much narrow and slit-like pores. The adsorption occurring in mesopores was associated with capillary condensation. The C value of BET equation interpreting the interaction energy between adsorbent and adsorbate molecules is indicative of microporosity of coconut shell-derived carbon. Over 95% of pore volume was located in micropores and mesopores for all activated carbons studied. Due to the difference in molecular structure among VOC species, only C_6H_6 adsorption signified the activated entry effect. The benzene adsorption on the activated carbon with high micropore volume was obviously temperature-dependent. An adsorption characteristic curve of peat-derived activated carbon was established for predicting the VOC adsorption capacities. Considering the heat of adsorption and the entropy change for each adsorption system, the physical adsorption was the predominant mechanism in the adsorption process. At high temperature, the benzene adsorption on bituminous coal and coconut shell-derived activated carbons increased which implied the enhancement of the interactions between benzene molecules and the activated carbon. Nevertheless, the increase from these interactions on adsorbed amount was negligible as compared to the actions of physical adsorption.

Acknowledgements

The authors express their sincere thanks to the National Science Council, Taiwan, ROC for its financial support (Contract no. NSC 86-2221-E-002-071) of this study.

References

[1] Gregg SJ, Sing KSW. Adsorption, surface area and porosity, 1st ed, London: Academic Press, 1967.
[2] de Boer JH. The structure and properties of porous materials, London: Butterworth, 1958.
[3] Zhdanov VP. Application of percolation theory to describing kinetic processes in porous solids. Adv Catal 1993;39:1–50.
[4] Sing KSW, Everett DH, Haul RAW, Moscou L, Pierotti RA, Rouquerol J, Siemieniewska T. Reporting physisorption data for gas/solid systems with special reference to the determination of surface area and porosity. Pure Appl Chem 1985;57(4):603–19.
[5] Lippens BC, de Boer JH. Studies on pore systems in catalysts V. The t-method. J Catal 1965;4:319–23.
[6] Mikhail RS, Brunauer S, Bodor EE. Investigations of a complete pore structure analysis. J Coll Inter Sci 1968;26:45–53.
[7] Horvath G, Kawazoe K. Method for calculation of effective pore size distribution in molecular sieve carbon. J Chem Eng Jap 1983;16:470–5.

[8] Tompkins FC. Chemisorption of gases on metals, New York: Academic Press, 1978.
[9] Gregg SJ, Sing KSW. Adsorption, surface area and porosity, 2nd ed, London: Academic Press, 1982.
[10] Chihara K, Suzuki M, Kawazoe K. Adsorption rate on molecular sieving carbon by chromatography. AIChE J 1978;24:237–45.
[11] Findenegg GH, Liphard M. Adsorption from solution of large alkane and related molecules onto graphitized carbon. Carbon 1987;25:119–28.
[12] Tsai WT. Study of activated carbon adsorption and catalyst combustion of VOCs. In: PhD thesis, Taipei, Taiwan: National Taiwan University, 1994.
[13] Chiang HL. Influences of physicochemical properties of activated carbon on VOC adsorption. In: PhD thesis, Taipei, Taiwan: National Taiwan University, 1995.
[14] Adamson AW. Physical chemistry of surfaces, New York: John Wiley, 1982.
[15] Smisek M. Active carbon: manufacture, properties and applications, New York: Elsevier, 1970.
[16] Jankowska H, Swiatkowski A, Choma J. Active carbon, New York: Ellis Horwood, 1991.
[17] Annual book of ASTM standards, vol. 15.05, Philadelphia, PA: American Society for Testing and Materials, 1996.
[18] Chiang PC. Effects of physicochemical characterizations of activated carbons on adsorption and/or desorption of hazardous air pollutants. In: Technical report, Taipei, Taiwan: National Science Council, 1998, NSC 86-2221-E-002-071.
[19] Warhurst AM, Fowler GD, McConnachie GL, Pollard SJT. Pore structure and adsorption characteristics of steam pyrolysis carbons from moringa oleifera. Carbon 1997;35:1039–45.
[20] Rodriguez-Reinoso F. The role of carbon materials in heterogeneous catalysis. Carbon 1998;36:159–75.
[21] McClellan AL, Harnsberger HF. Cross-sectional areas of molecules adsorbed on solid surfaces. J Coll Inter Sci 1967;23:577–99.